



OPEN

Enhancement of melanoma aggressiveness via p38-MAPK, HIF-1 α pathways, and metabolic reprogramming induced by *Candida albicans*

Leire Aparicio-Fernandez¹, Nahia Cazalís-Bereicua¹, Maialen Areitio¹, Oier Rodriguez-Erenaga¹, Lucia Abio-Dorronsoro¹, Leire Martín-Souto¹, Idoia Buldain², Joana Márquez³, Aitor Benedicto⁴, Beatriz Arteta³, Nuria Macías-Cámar⁵, Monika González⁵, Jose Ezequiel Martín Rodríguez⁵, Ana M. Aransay^{5,6}, Aize Pellon^{5,7}, David L. Moyes⁷, Juan Anguita^{5,8}, Aitor Rementeria¹, Aitziber Antoran¹✉ & Andoni Ramírez-García¹

Recent studies have increasingly focused on the role of fungi, including *Candida albicans*, in carcinogenesis. Since *C. albicans* is a component of the human microbiota, particularly on the skin, we investigated its effect on the phenotype and signalling pathways of melanoma cells. Assays for migration, adhesion, angiogenesis, and hepatic metastasis showed that *C. albicans* promotes a more malignant phenotype in melanoma cells. At the transcriptomic level, *C. albicans* increased the expression of VEGF (*Vegfa*), and genes associated with MAPK and HIF-1 signalling pathways, and with aerobic glycolysis. Further in vitro analysis revealed that TLRs and EphA2 receptors are involved in the recognition of live *C. albicans*, stimulating VEGF secretion and expression of the AP-1 transcription factor component c-Fos through p38-MAPK and HIF-1 α . These pathways also regulate the expression of other AP-1 constituents such as *Atf3*, *Jun*, and *Jund*. Moreover, p38-MAPK regulates glycolytic genes like *Hk2*, *Slc2a1*, and *Eno2*. In conclusion, *C. albicans* activates the p38-MAPK/c-Fos/AP-1 and HIF-1/HIF-1 α /c-Fos/AP-1 pathways in melanoma cells, promoting a pro-angiogenic environment and metabolic reprogramming. Therefore, this study clarifies the impact of *C. albicans* on melanoma cells, which can lead to the use of antifungal therapies as complementary to traditional treatments for melanoma.

Keywords Melanoma, *Candida*, Angiogenesis, Metabolism, Cancer, Metastasis

Cancer is one of the main causes of death worldwide, resulting in approximately 10 million deaths in 2020 alone¹. It is estimated that between 13% and 18% of these cases are caused by microorganism infections^{2,3}. In fact, the International Agency for Research on Cancer (IARC) has already classified thirteen microorganisms as carcinogenic, including viruses, bacteria, and parasites⁴. However, recent studies have shown that other microorganisms could also directly promote cancer. While most studies focus on virus and bacteria interactions

¹Department of Immunology, Microbiology and Parasitology, Faculty of Sciences and Technology, University of the Basque Country (UPV/EHU), Leioa, Spain. ²Department of Immunology, Microbiology and Parasitology, Faculty of Pharmacy, UPV/EHU, Vitoria-Gasteiz, Spain. ³Department of Cell Biology and Histology, Faculty of Medicine and Nursery, UPV/EHU, Leioa, Spain. ⁴Department of Cell Biology and Histology, Faculty of Pharmacy, UPV/EHU, Vitoria-Gasteiz, Spain. ⁵Center for Cooperative Research in Biosciences (CIC bioGUNE), Basque Research and Technology Alliance (BRTA), Derio, Spain. ⁶Centro de Investigación Biomédica en Red de Enfermedades Hepáticas y Digestivas (CIBERehd), Instituto de Salud Carlos III, Madrid, Spain. ⁷Centre for Host-Microbiome Interactions, Faculty of Dentistry, Oral & Craniofacial Science, King's College London (KCL), London, UK. ⁸Ikberasque, Basque Foundation for Science, Bilbao, Spain. ✉email: aitziber.antoran@ehu.eus

with cancer, some research also highlights a link between cancer progression and certain fungi, such as *Malassezia*, *Aspergillus fumigatus* and *Candida albicans*^{5–7}.

C. albicans is an opportunistic dimorphic fungus that is usually part of the human microbiota in many locations, such as the oral cavity, gastrointestinal tract, or vagina⁸. However, in the last decades, it has been suggested that it could promote cancer initiation and progression. Cawson in 1969 was the first who related *Candida* presence with promotion of cancer, specifically leukoplakia, which is a precancerous oral lesion⁹. Since then, many studies have described its association especially with oral and oesophageal cancer in humans^{10,11}, but also with other types of cancers and metastasis^{5–7,12}. Nevertheless, the mechanisms by which *C. albicans* can induce cancer progression and metastasis have not been completely elucidated. It has been proposed that production of carcinogenic compounds such as acetaldehyde or nitrosamine, chronic inflammation, or induction of metastasis could play a role^{13,14}.

In this context, it has been demonstrated that *C. albicans* can induce cellular processes associated with cancer including enhanced cell migration, the production of oncometabolites, and the activation of pro-inflammatory cytokines and the expression of cancer-related genes in various cell lines in vitro^{7,11,15,16}. Moreover, in vivo oral cancer models have also linked *C. albicans* to augmented cancer development and progression^{11,17}. These results are supported by in vivo research conducted by our group employing melanoma cells, a particularly aggressive cancer type, which revealed that *C. albicans* increases liver metastasis and creates a pro-metastatic microenvironment characterized by an enhanced release of Tumor Necrosis Factor (TNF) and Interleukin-18 (IL-18)^{18–20}. Consistent with these findings, Szóstak and colleagues recently reported that gut *C. albicans* is strongly associated with accelerated melanoma progression²¹, potentially through direct fungal–melanoma cell interactions.

Therefore, given that *C. albicans* can colonize the skin as well as cause systemic infections²², it has the potential to interact directly with melanoma cells either at the primary tumor site or during dissemination in the bloodstream, where both can coexist. Despite this possibility, the direct effect of *C. albicans* on melanoma aggressiveness remains unexplored. Based on these findings, we hypothesize that *C. albicans* may directly drive melanoma progression by activating pro-tumorigenic and pro-metastatic pathways in melanoma cells. In consequence, the aim was to examine the role that this opportunistic fungus plays in promoting the development of cancer, particularly melanoma, and the identification of molecular pathways and mediators involved. Using in vitro and in vivo techniques we demonstrate that *C. albicans* induces phenotypic changes and metabolic reprogramming in melanoma cells, increasing their aggressiveness through activation of inflammatory, pro-angiogenic, and hypoxic pathways, specifically p38-MAPK/c-Fos and HIF-1α/c-Fos. These findings support the development of new therapies for melanoma cases influenced by *C. albicans*.

Results

C. albicans stimulates migration, adhesion, pro-angiogenesis, and hepatic metastasis, but no proliferation, in melanoma cells

In vitro assays revealed that live and heat-killed (HK)-*C. albicans* yeasts promoted a significant increase in the migration ability of melanoma cells ($P=0.006$ and $P=<0.001$ for MOI (Multiplicity Of Infection) 0.25 and 0.5 against the control, respectively; Fig. 1a) and their adhesion capacity to liver sinusoidal endothelial cells (LSECs) ($P=0.006$; Fig. 1b), respectively. Furthermore, a significant increase in the migration capacity of LSECs was observed when they were incubated with conditioned media obtained from melanoma cells exposed to live *C. albicans*, which could indicate the presence of pro-angiogenic substances in the media ($P=0.012$; Fig. 1c). However, HK-*C. albicans* yeast failed to increase melanoma cell proliferation (Supplementary Fig. 1).

In addition to the in vitro assays, the pro-metastatic effect induced by *C. albicans* was determined by intrasplenic inoculation in mice of melanoma cells previously stimulated with live *C. albicans*. After 14 days, all mice injected with melanoma cells developed hepatic metastasis. As shown in Fig. 1d, melanoma cells formed multiple pigmented foci in the liver, varying in extension and definition, without a clear delimitation. Consequently, the macroscopic measurement was expressed as the percentage of the liver area occupied by these foci. A significantly larger affected area was observed in livers from mice inoculated with *C. albicans*-stimulated melanoma cells compared to those receiving non-stimulated cells ($P=0.001$; Fig. 1d). The area occupied by metastatic cells was also measured microscopically. In this analysis, the size of the tumor tissue area was significantly greater in mice injected with *C. albicans*-stimulated melanoma cells compared to control mice ($140.4 \pm 30.1 \text{ mm}^2$ vs. $106.3 \pm 32.9 \text{ mm}^2$, respectively; $P=0.011$; Fig. 1e).

Transcriptional response of melanoma cells to *C. albicans* stimulation

The study of the mechanisms underlying the alterations of the phenotype induced by *C. albicans* was first carried out through a transcriptomic analysis of melanoma cells exposed to live fungal cells (MOI 1) for six hours. The results showed 63 genes significantly ($| \text{FC} | > 1.5$, $p_{\text{adj}} < 0.05$) upregulated while no genes were downregulated in comparison to melanoma cells not exposed to the fungus (Fig. 2a, Supplementary Dataset File 1). Notably, among the differentially-expressed genes (DEGs), genes involved in signaling pathways (*Dusp1*, *Dusp8*, *Trib3*), glucose metabolism (*Hk2*, *Slc2a1*, *Pdk1*), and transcription factors (*Jun*, *Fos*, *Atf3*) were upregulated. In addition, 54% of the genes (34 out of 63) and nine of the first 15 Gene Ontology-Biological Processes (GO-BPs; ordered according to the GeneRatio) were associated with a response to stress conditions, of which four GO-BPs were specifically related to hypoxia (Fig. 2b). With respect to KEGG analysis, only three pathways were significantly upregulated in response to *C. albicans*: MAPK signaling pathway (mmu04010), HIF-1 signaling pathway (mmu04066), and renal cell carcinoma (mmu05211) (Fig. 2c). Interestingly, these three pathways share the gene *Vegfa*, which codes for the pro-angiogenic vascular endothelial growth factor (VEGF) (Fig. 2d).

A second less restrictive bioinformatics analysis of the results was performed, this time only considering the $p_{\text{adj}} (< 0.05)$ as a selecting parameter to give a more extensive view of the pathways activated. Using this parameter,

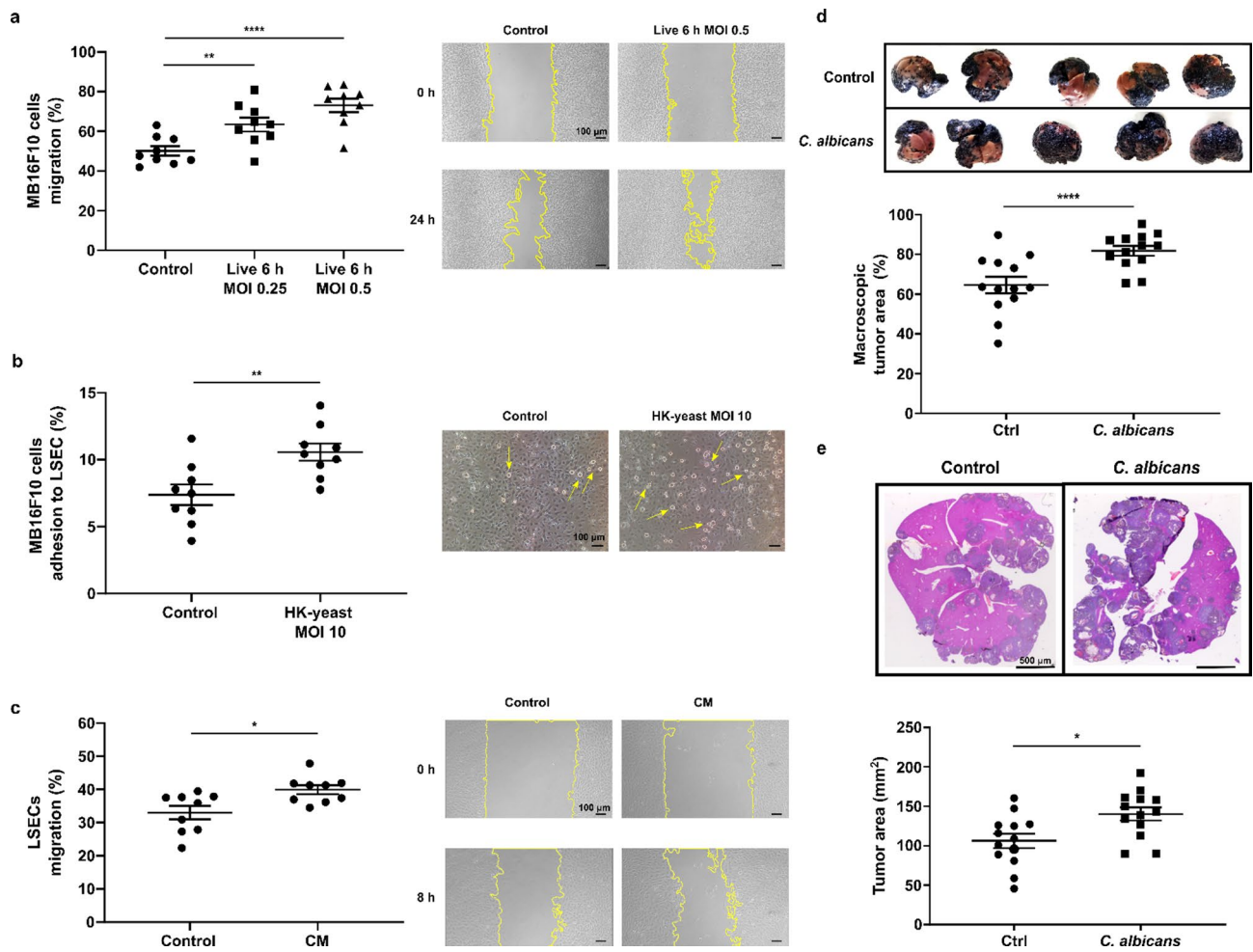


Fig. 1. *Candida albicans* effect in melanoma cells phenotype. Melanoma cells migration after 24 h of exposure for six hours to (a) live-*C. albicans* yeast MOI 0.25 and 0.5 or (b) Heat-Killed (HK)-*C. albicans* yeast MOI 10. (c) LSECs migration after eight hours of exposure to the conditioned media (CM) collected from melanoma cells exposed to live *C. albicans* MOI 5 of the fungus for six hours. (a–c) graphs represent all the results obtained and images (10X magnification) are representative of one experiment of each assay ($n=9$ technical replicates from 3 biologically independent samples). Scale bars 100 μ m. (d,e) Effect of *C. albicans* stimulation of melanoma cells on liver metastasis promotion ($n=13$ biologically independent samples): (d) Representative macroscopic liver images, and graphical representation of liver area occupied by metastatic melanoma in control group mice and *C. albicans*-stimulated melanoma cells receiving mice. (e) Representative H&E staining of metastatic colonization, and microscopic tumor area size (in mm^2) per 200 mm^2 of liver section in control group and *C. albicans*-stimulated melanoma cells injected group. Scale bar 500 μ m. Data were presented as the individual values, means \pm SEM. Two-tailed unpaired Student's t test was used to examine the statistical significance between groups. *, **, and **** denote $P<0.05$, $P<0.01$, and $P<0.001$, respectively.

271 upregulated genes (Supplementary Dataset File 2) were detected, several of them being involved in the HIF-1 signaling pathways, central carbon metabolism in cancer (mmu05230), pathways in cancer (mmu05200), and MAPK signaling pathways. Of note, gene expression of some kinases (*Map2k1*, *Map3k1* or *Mknk2*), signaling regulators (e.g. *Dusp2*, *Dusp4*) or glycolytic enzymes (e.g. *Eno2*, *Ldha*) were found to be upregulated using these settings (Fig. 2e).

C. albicans drives a response in melanoma cells that leads to VEGF release

We next investigated the effects of fungal morphology, viability, and conditioned media on melanoma cells in greater detail. For that, the release of the pro-angiogenic molecule VEGF and the expression of the *Fos* gene, an important MAPK-related transcription factor overexpressed in the transcriptomic analysis, were quantified by ELISA (Enzyme-Linked Immuno Sorbent Assay) and RT-qPCR respectively (Fig. 3a, b). The highest levels of VEGF release ($P=0.030$; Fig. 3a) and *Fos* expression (Fig. 3b) were observed after the co-incubation of cancer cells with live *C. albicans*. The rest of the conditions promoted a lesser, statistically non-significant increase in VEGF, and barely altered the expression of the *Fos* gene ($P=0.014$ for HK-hyphae). Thus, for subsequent experiments only live *C. albicans* was used.

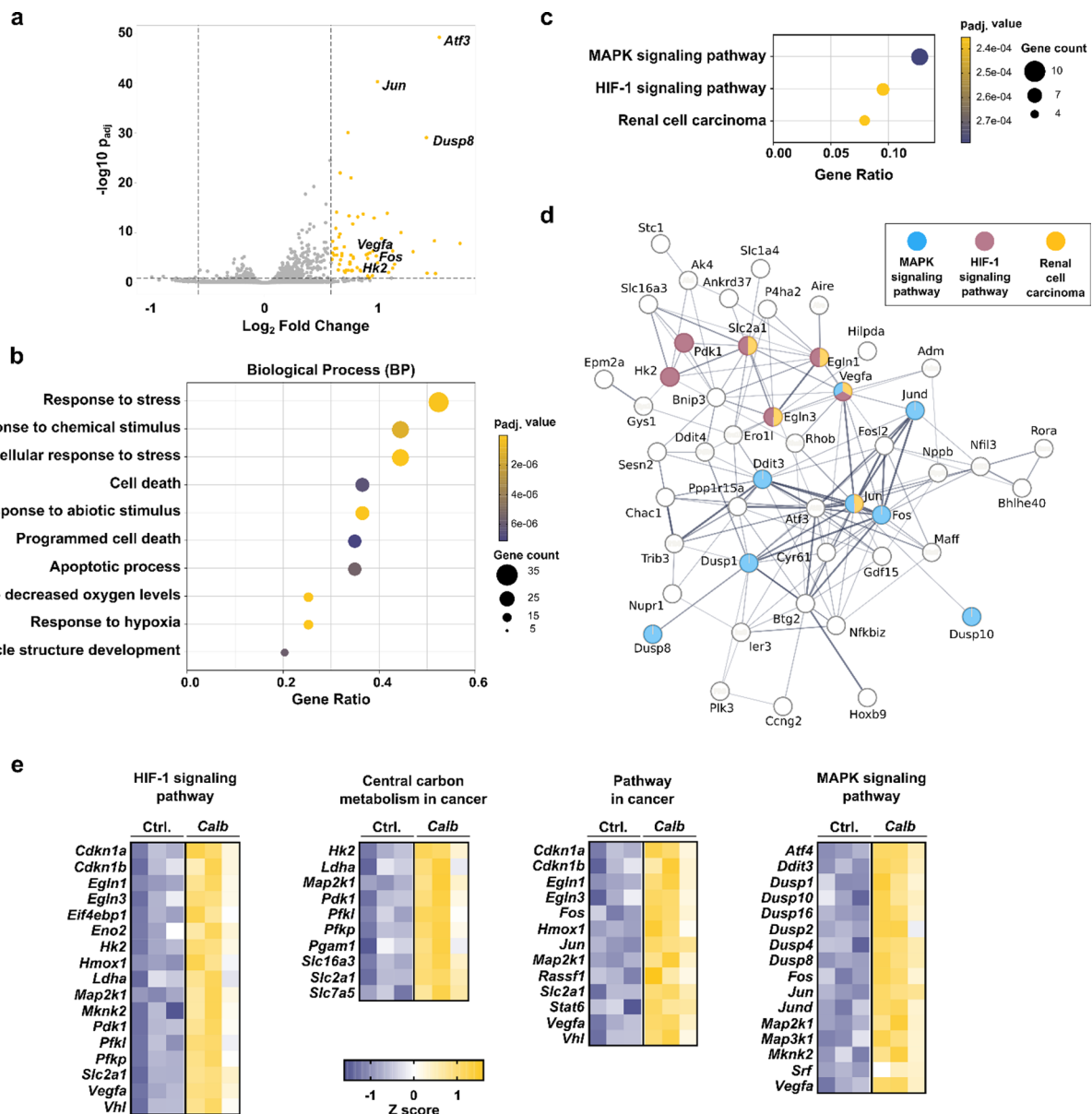


Fig. 2. Transcriptomic analysis of melanoma cells exposed to live *Candida albicans* at MOI 1 for six hours. (a) Volcano plot representing differentially-expressed genes (DEGs). Yellow dots represent upregulated genes. (b) GO enrichment analysis of the Biological Processes (GO-BP) significantly upregulated. (c) KEGG pathways significantly upregulated. (d) STRING performed with upregulated genes, their relationship (grey lines) and the KEGG pathways in which they are implicated (only interrelated genes are shown). Line thickness indicates the strength of data support. (e) Heatmaps showing the expression levels comparison between samples (Z-score) of DEGs: HIF-1 signaling pathways, central carbon metabolism in cancer, pathways in cancer and MAPK signaling pathways. Each column represent a biologically independent sample. Yellow and purple boxes represents upregulated and downregulated genes, respectively. (a-d) analysis were performed for $| FC | > 1.5$ and $p_{adj} \leq 0.05$ and, (e) analysis with $p_{adj} \leq 0.05$ (iDEP 1.0 tool and Deseq2 method) ($n=3$ biologically independent samples).

To investigate the initial host-fungus contact that activates the melanoma cell response, the role of the primary receptors involved in host-*Candida* interactions, mainly pattern recognition receptors (PRRs), were studied. Molecular inhibitors for the receptors EGFR and EphA2, and for the signal transducing proteins for almost all TLRs (MyD88) and CLRs (Syk), were used to assess their effects on VEGF release and c-Fos protein expression (Fig. 3c-e). The inhibition of MyD88-mediated TLRs signal transduction resulted in a considerable reduction of VEGF release induced by *C. albicans* ($P=0.074$) but did not show any effect on c-Fos protein expression, which appeared to be mainly mediated by the β -glucan receptor EphA2. However, inhibition of both Syk and EGFR did not alter any of the two parameters analyzed.

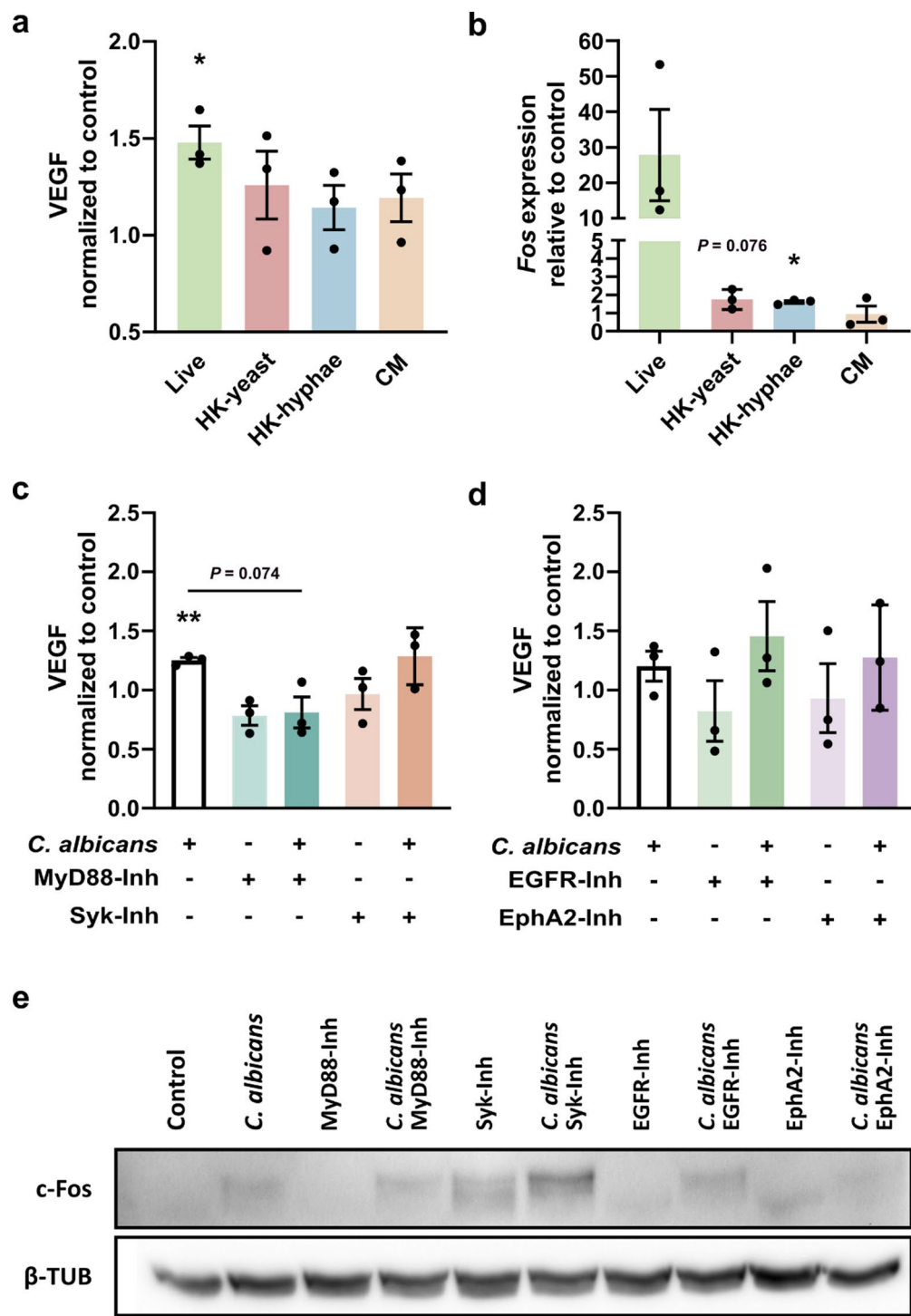


Fig. 3. Influence of the viability of *Candida albicans* and the main pathogen recognition receptors (PRRs) in melanoma cells after six hours of stimulation. (a) VEGF release and (b) *Fos* gene expression induced by different morphologies and released molecules of *C. albicans*. (c,d) VEGF release and (e) c-Fos protein expression in live *C. albicans*-exposed melanoma cells alone or treated with inhibitors for c, e TLRs (MyD88 inhibitor: TJ-M2010-5, 30 μ M) and CLRs (Syk inhibitor: Piceatannol, 30 μ M), and (d,e) EGFR (PD153035, 1 μ M) and EphA2 (NVP-BHG712, 1 μ M). (a-d) Data were presented as the individual values, means \pm SEM ($n = 3$ biologically independent samples). Two-tailed unpaired Student's t test was used to examine the statistical significance between groups. * and ** denote $P < 0.05$ and $P < 0.01$ in comparison to control without *C. albicans*, respectively. (e) Representative data of three independent Western Blots. HK: Heat-Killed; CM: Conditioned Media obtained after six hours of exposure of melanoma cells to live *C. albicans* MOI 5.

The release of VEGF by melanoma cells in response to *C. albicans* is mediated by p38-MAPK and HIF-1 α

To decipher the signal cascade induced by *C. albicans* in melanoma cells, the impact on VEGF release of the three main pathways activated by MAPK (ERK1/2, JNK and p38), and the inflammation-related NF- κ B pathway, was studied using different inhibitors for p38, JNK, ERK1/2 and NF- κ B (Fig. 4a). The results demonstrated a significant reduction in VEGF release in cells stimulated by *C. albicans* when p38-MAPK was inhibited ($P=0.038$), whereas no alterations were observed with the inhibitors for ERK1/2, JNK, or NF- κ B.

The involvement of the HIF-1 signaling pathway, identified as the second pathway in the KEGG analysis, in VEGF release was then studied using a specific HIF-1 α inhibitor (Fig. 4b). The data revealed a significant reduction in VEGF release in cells stimulated with *C. albicans* when treated with the inhibitor ($P=0.008$), compared to those without inhibitor treatment, indicating that, in addition to p38-MAPK, HIF-1 α regulates VEGF release induced by *C. albicans*.

Previous work has identified c-Fos as a central component in the MAPK signaling circuit activated by *C. albicans* infection of epithelial cells^{23,24}. Thus, we next set out to determine whether p38-MAPK and HIF-1 α inhibition impacted on c-Fos gene and protein expression in melanoma cells. Inhibition of both pathways demonstrated a significant reduction of *Fos* gene ($P=0.007$ and $P=0.020$ for p38-MAPK and HIF-1 α inhibition, respectively) and c-Fos protein expression in cells infected with *C. albicans* (Fig. 4c-e). However, neither of them alone reduced its gene and/or protein expression to control levels, suggesting that they are independently involved in c-Fos production.

Given the central role played by p38-MAPK in regulating VEGF release, we investigated whether activation of the MAPK-activated c-Fos/AP-1 transcription factor component plays a role in VEGF production and release (Fig. 4f). As expected, the inhibition of the c-Fos-containing AP-1 transcription factor (c-Fos/AP-1) resulted in a substantial decrease in the VEGF release in the presence of *C. albicans* with respect to the cells stimulated with the fungus without the inhibitor ($P=0.097$), confirming that the c-Fos/AP-1 complex is, at least in part, responsible for VEGF production.

The release of VEGF by melanoma cells in response to *C. albicans* is mediated by the AP-1 transcription factor

The dimeric transcription factor AP-1 is formed by proteins from the Fos, Jun, ATF, and MAF families²⁵. Our transcriptomic analysis revealed that, in addition to *Fos*, *C. albicans* exposure induced the expression of the, *Jund*, *Jun* and *Atf3* genes comparing to the control ($P=0.004$, $P=0.008$ and $P=0.052$, respectively). Thus, the involvement of the p38-MAPK and HIF-1 α in regulating the activation of these genes was investigated (Fig. 5).

The results showed that the gene expression of all three genes and particularly *Jund* was reduced by p38-MAPK inhibition ($P=0.001$ for *Jund* expression) and, to a lesser extent, by HIF-1 α inhibition ($P=0.022$ for *Jund* expression). These results suggest that proteins encoded by these genes in addition to *Fos* may also form the AP-1 complex that activates VEGF secretion induced by *C. albicans*, and that both p38-MAPK and HIF-1 α are involved in AP-1 activation, although other processes may also take part.

Central carbon metabolism is altered in melanoma cells due to *C. albicans* stimulation

To confirm the metabolic reprogramming induced by *C. albicans* in melanoma cells suggested by the transcriptomic analysis, Extracellular Acidification Rate (ECAR) analyses were performed. The results showed a significant acidification of the media after six hours when the cells were exposed to *C. albicans*, which is potentially a consequence of an increase in aerobic glycolysis ($P=0.032$; Fig. 6a).

The interconnection between these metabolic changes and the pro-angiogenic VEGF release induced by *C. albicans* was further studied using molecular inhibitors for the glucose transporter GLUT1 (coded by *Slc2a1* gene) and the glycolytic enzyme hexokinase (HK2). Inhibition using either of the two inhibitors, GLUT1 and HK2, significantly decreased *C. albicans*-induced VEGF release in melanoma cells ($P=0.022$ and $P=0.007$, respectively; Fig. 6b).

Finally, to determine the influence of p38-MAPK and HIF-1 α on metabolic reprogramming, the expression of the genes *Eno2*, *Hk2* and *Slc2a1* was analyzed after inhibition of both pathways. Inhibition of p38-MAPK resulted in a reduction in expression of all three genes, with statistically significant differences for *Eno2* and *Hk2* ($P=<0.001$ and $P=0.011$, respectively; Fig. 6c-e). Conversely, HIF-1 α inhibition did not significantly inhibit gene expression of any of the three genes (Fig. 6f-h). These results suggest that p38-MAPK activation drives metabolic reprogramming while the HIF-1 α does not.

Discussion

Microbial infections have been associated with cancer development and progression, with most of the research focusing on viruses and bacteria, while fungi remain overlooked. Despite this, an increasing number of studies have highlighted the role of fungi in cancer, in particular *C. albicans*^{5,6}. *C. albicans* is a commensal fungus often found in the human mycobiota of the skin, among other areas²², where one of the most aggressive and deadly tumors, melanoma, develops²⁶. The aim of this study was to investigate the impact of *C. albicans* presence on cells from this type of cancer.

According to the latest “Hallmarks of Cancer” proposed by Douglas Hanahan²⁷, tumor cells acquire a range of capabilities essential for developing malignant phenotypes, such as uncontrolled proliferation and augmented invasiveness, among others. In this regard, our results showed an increase in adhesion to LSECs as well as migratory capacity of *C. albicans*-exposed melanoma cells, although no increase in their proliferation was observed. These results are in line with the results obtained by Vadovics et al.¹¹ for oral squamous cell carcinoma (OSCC) cell lines. Furthermore, LSECs exposed to supernatants obtained from live *C. albicans*-stimulated melanoma cells showed a significantly increased migratory capacity. This pro-angiogenic capacity

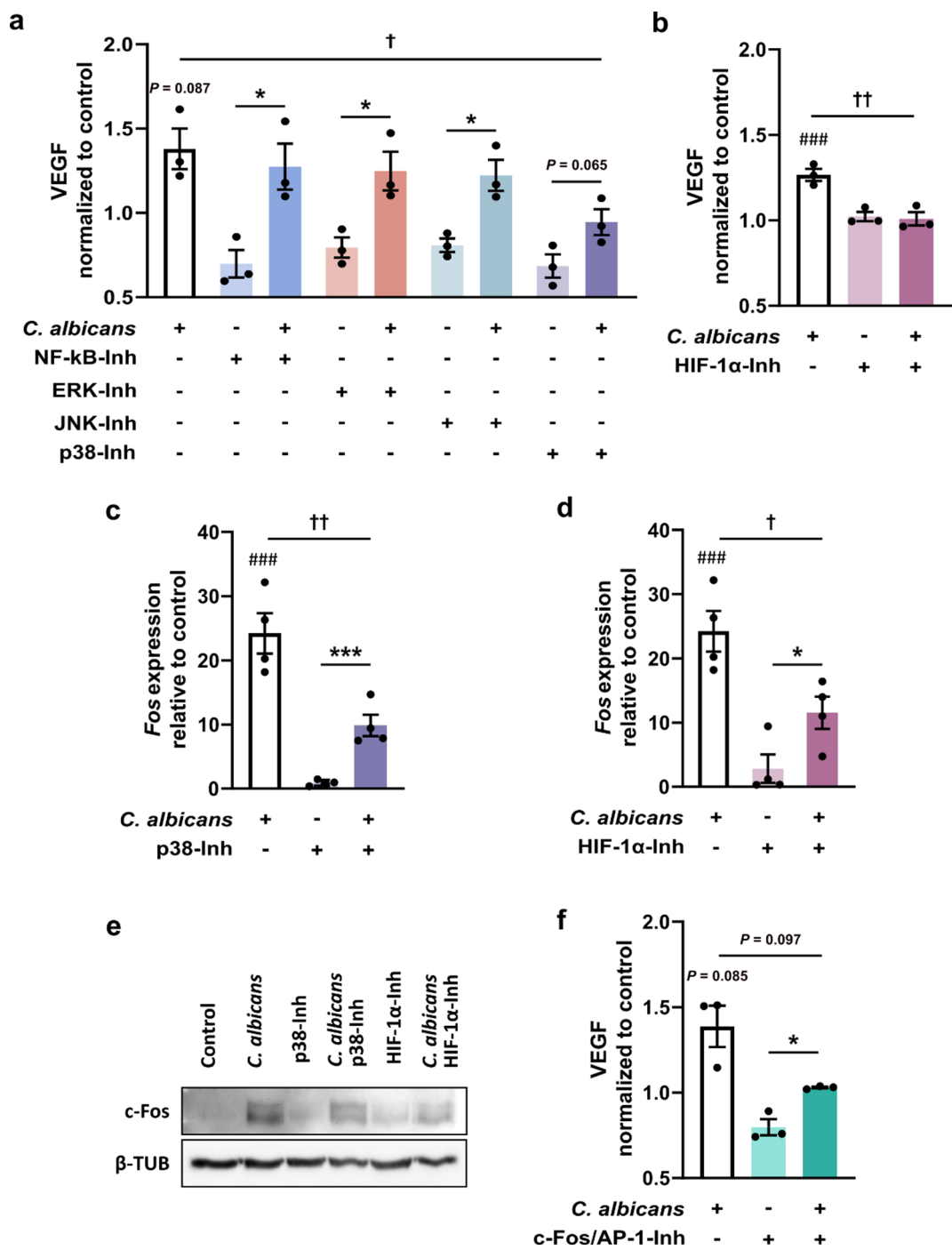


Fig. 4. Live *Candida albicans* at MOI 5 regulates MAPK and HIF-1 α pathways in melanoma cells. VEGF release induced by six hours of stimulation with *C. albicans* in absence and presence of inhibitors for (a) NF- κ B (BAY 11-7082, 2 μ M), ERK1/2 (PD-0325901; 1 μ M), JNK (SP600125, 10 μ M), p38 (SB 203580, 10 μ M), (b) HIF-1 α (LW6, 10 μ M) and c Fos/AP-1 complex (T-5224, 10 μ M). (c,d) Melanoma cells Fos gene and (e) protein expression analysis in absence or presence of p38 inhibitor or HIF-1 α inhibitor. (f) VEGF release induced by six hours of stimulation with *C. albicans* in absence and presence of inhibitors for c-Fos/AP-1 complex (T-5224, 10 μ M). Data were presented as the individual values, means \pm SEM. (a,b,f) ($n=3$ biologically independent samples); (c,d) ($n=4$ biologically independent samples). Two-tailed unpaired Student's t test was used to examine the statistical significance between groups. $^{###}$ denotes $P < 0.005$ respect to control without *C. albicans*; * and *** denote $P < 0.05$ and $P < 0.005$ of each inhibitor compared to inhibitor with *C. albicans*, respectively; \dagger , \ddagger and $\ddagger\ddagger$ denote $P < 0.05$, $P < 0.01$ and $P < 0.005$ of *C. albicans* group compared to inhibitors with *C. albicans* groups, respectively. (e) Representative data of three independent Western Blots. HK: Heat-Killed; CM: Conditioned Media obtained after six hours of exposure of melanoma cells to live *C. albicans* MOI 5.

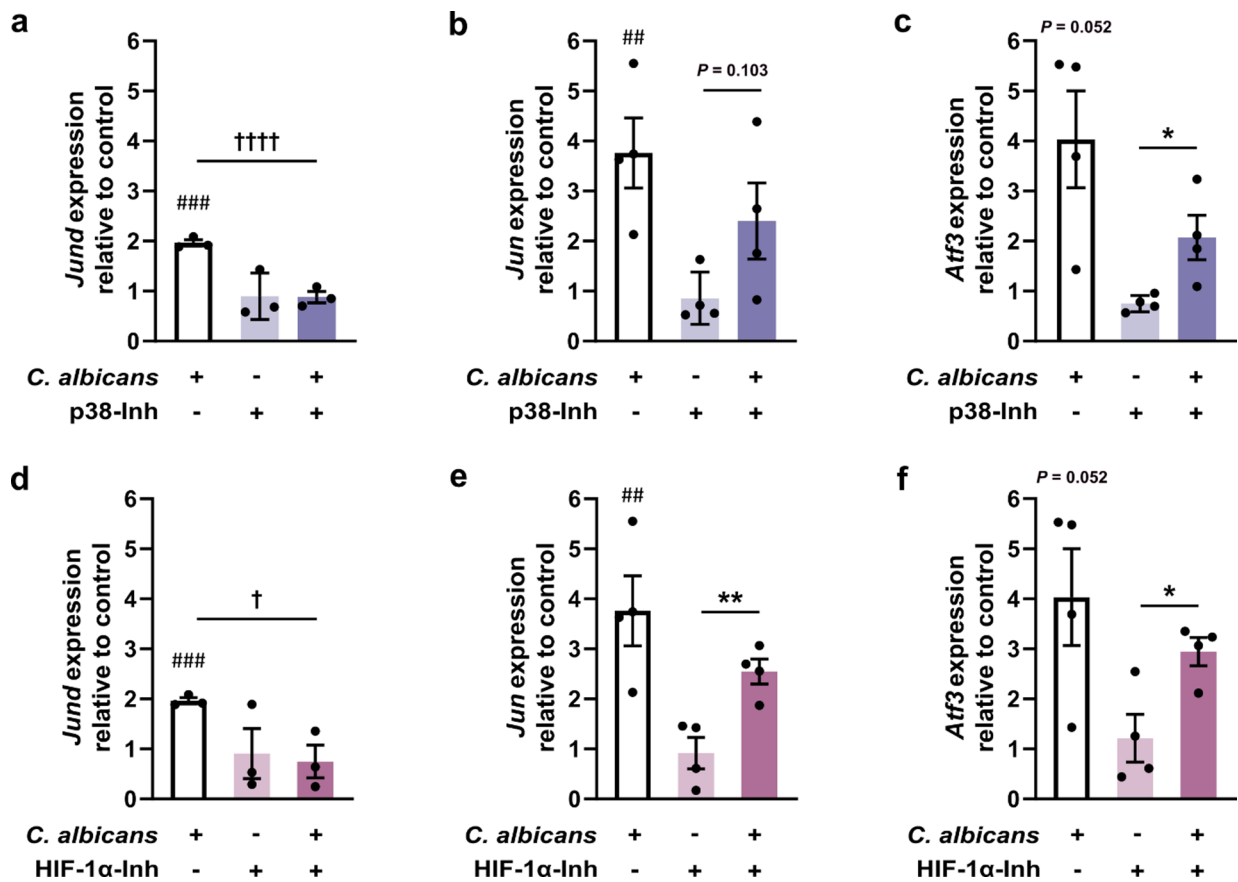


Fig. 5. Analysis of AP-1 transcription factor activation by MOI 5 live *Candida albicans* in melanoma cells. Gene expression of *JunD*, *Jun* and *Atf3* induced by six hours of stimulation with *C. albicans* alone or treated with (a-c) p38 inhibitor or (d,f,g) HIF-1 α inhibitor. Data were presented as the individual values, means \pm SEM. (a,d) ($n=3$ biologically independent samples); (b,c,e,f) ($n=4$ biologically independent samples). Two-tailed unpaired Student's t test was used to examine the statistical significance between groups. ## and ### denote $P<0.01$ and $P<0.005$ respect to control without *C. albicans*, respectively; * and ** denote $P<0.05$ and $P<0.01$ of each inhibitor compared to inhibitor with *C. albicans*, respectively; † and †††† denote $P<0.05$ and $P<0.001$ *C. albicans* group compared to inhibitors with *C. albicans* groups, respectively.

could be caused by the production of growth factors and cytokines (i.e., VEGF, bFGF, IL-8, or angiopoietin) by melanoma cells²⁸.

In accordance with our in vitro data, pre-incubation of melanoma cells with *C. albicans* enhanced their metastatic capacity in an in vivo murine model of metastatic progression, increasing macro- and microscopic hepatic metastatic area. These results are in line with previous studies in which mice injected with both melanoma cells and *C. albicans* presented an augmented liver metastasis and increased TNF and IL-18 release, in comparison to mice injected only with melanoma cells¹⁸. Moreover, studies with OSCC mouse models suggested that *C. albicans* can initiate cancer and contribute to its progression and development in vivo^{11,17}.

Once we observed the phenotypical effects exerted by *C. albicans* in vitro and in vivo, a transcriptomic analysis of melanoma cells revealed that they respond to *C. albicans* primarily by activating the MAPK and HIF-1 signaling pathways. Exposure to *C. albicans* led to the overexpression of several MAPK-related components, including kinases, transcription factors and signaling regulators, as well as metabolic genes associated with hypoxia, such as glycolytic enzymes, glucose transporters, lactate production, and tricarboxylic acid cycle inhibitors. Remarkably, only one overexpressed gene, the pro-angiogenic VEGF, connected all these pathways, highlighting its potentially pivotal function in this response. These results are consistent with previous studies showing overexpression of immune-response pathways, particularly NF- κ B and MAPK regulators, as well as induction of oxidative phosphorylation-related genes, at this and earlier time points, in other epithelial and endothelial cells^{16,23,29–33}. These studies also reported that at later stages (12–24 h), cells exhibited transcriptional signatures of damage and defense responses, including apoptosis, alongside an exacerbated immune response driven by fungal invasion^{29,34}.

Subsequently, we investigated whether the activation of melanoma cells by *C. albicans* depends on fungal morphology, viability, or molecules released by the fungus. We examined the release of VEGF and gene expression of *Fos*, which was also found overexpressed in the transcriptomic data and extensively reported in the response to *C. albicans* hyphae^{23,30,33}. The highest increase in both cases was induced by live *C. albicans*,

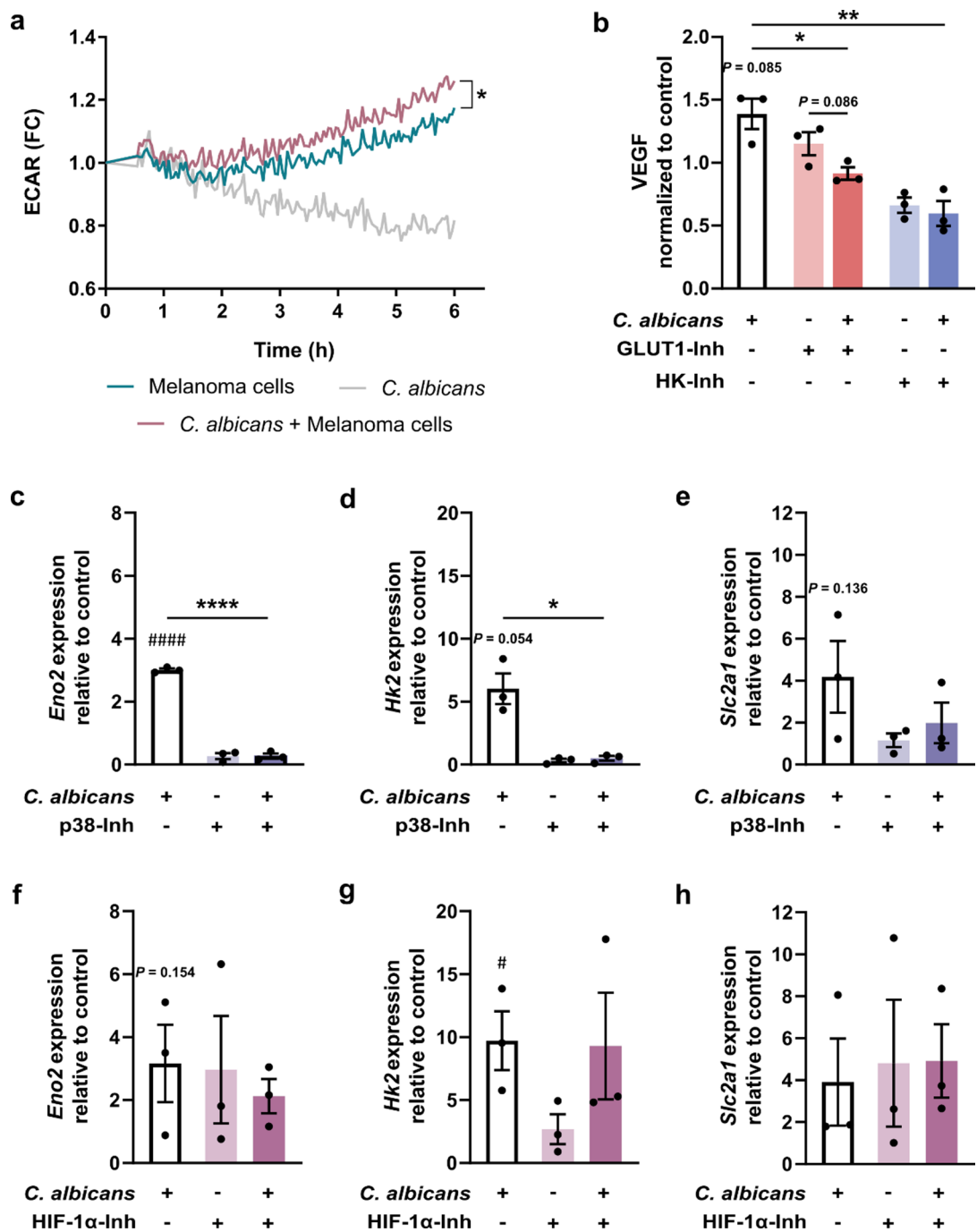


Fig. 6. Analysis of metabolic changes induced by live *Candida albicans* in melanoma cells. (a) Extracellular Acidification Rate (ECAR) of melanoma cells in controls and in cell in contact with *C. albicans* for six hours. Data shown as the mean of the fold change (FC) of initial fluorescence values in four independent experiments. (b) VEGF release induced by six hours of stimulation with *C. albicans* alone or in presence of glucose transporter 1 (GLUT1) inhibitor (BAY-876; 25 nM) and hexokinase (HK) inhibitor (2-DG; 5 mM). Gene expression of *Eno2*, *Hk2* and *Slc2a1* induced by six hours of stimulation with *C. albicans* alone or in presence of (c–e) p38 inhibitor (SB 203580, 10 μ M) or (f–h) HIF-1 α inhibitor (LW6, 10 μ M). Data were presented as the individual values, means \pm SEM. a ($n=4$ biologically independent samples); (b–g) ($n=3$ biologically independent samples). (a,c,d) ($n=4$ biologically independent samples; (b,f) ($n=3$ biologically independent samples). Two-tailed unpaired Student's t test was used to examine the statistical significance between groups. # and ##### denotes $P<0.05$ and $P<0.0001$ respect to control without *C. albicans*, respectively; * and *** denote $P<0.05$ and $P<0.005$ of each inhibitor compared to inhibitor with *C. albicans*, respectively.

indicating that fungal viability is important for the process. This viability allows morphological changes that can increase its virulence²³ and to secrete proteins or toxins like Candidalysin which may trigger an inflammatory response specifically linked to activation of the MAPK/c-Fos pathways^{31,35}. This is also consistent with the reduced virulence of yeast-locked *C. albicans* mutants exhibited in mice³⁶, and the lack of response of epithelial cells to HK-yeasts²³. Therefore, further studies were performed using live *C. albicans* yeast.

Investigation of the involvement of several receptors, mainly PRRs, already linked to *C. albicans* recognition, including TLRs, CLRs, EGFR, and EphA2^{32,37}, in the responses described here indicated that only the inhibition of MyD88-dependent TLRs (all TLRs, except TLR3) significantly reduced VEGF release. These results support the role of TLRs not only in recognition of *C. albicans* by melanoma cells, but also in MAPK/AP-1 activation and subsequent VEGF release, as previously observed³⁸. However, our results demonstrated that while c-Fos/AP-1 inhibition reduced VEGF release, c-Fos protein expression is not essential for TLR-initiated VEGF secretion. This suggests that TLRs may activate other components of the AP-1 complex. In fact, AP-1 is a dimeric transcription factor widely related to cancer development that can be composed of different proteins from the Fos, Jun, ATF, and MAF families²⁵.

In contrast, EphA2 inhibition completely suppressed c-Fos protein expression, which is consistent with EphA2 role in activating inflammatory responses against *C. albicans* via the c-Fos/AP-1 pathway³⁹. However, no effect on VEGF release was observed. Therefore, although it cannot be ruled out that c-Fos may play a role in *C. albicans*-induced VEGF release conforming AP-1 heterodimers with other proteins from the families abovementioned (i.e., c-Jun)²⁵, these findings suggest that AP-1 homo/heterodimers that do not include c-Fos may be enough to drive VEGF production in melanoma cells. Taking all this into account, we propose that *C. albicans* recognition by TLRs stimulates the activation of different AP-1 complex proteins, which subsequently leads to VEGF release. In contrast, EphA2 receptor activity appears to activate c-Fos, which needs additional components to form functional heterodimers of AP-1 to stimulate VEGF production.

Next, we analyzed the effect of the two main pathways enriched in our transcriptomic analyses on VEGF release, namely the MAPK pathways (specifically the ERK1/2, JNK and p38) and HIF-1 (specifically the HIF1 α subunit). In addition to them, the NF- κ B pathway was included, as various cell types respond to *C. albicans* through its activation^{23,30,40,41}. Of all of them, we found that only inhibition of the p38-MAPK and HIF-1 α , but not ERK1/2, JNK, or NF- κ B, led to a significant reduction in VEGF release from melanoma cells stimulated with *C. albicans*. These results agree with previous studies indicating that the p38-MAPK drives VEGF production through the formation of AP-1 complexes in different cell lines^{38,42}, whilst HIF-1 α is a well-established promoter of VEGF release⁴³. Additionally, it has been already stated that the abovementioned TLRs induce activation of p38-MAPK and c-Fos after *C. albicans* recognition^{23,44}. Moreover, Roselletti et al.⁴⁵ showed that *C. albicans*-hyphae carriers with vaginal candidiasis exhibited enhanced expression of TLR2, TLR4 and EphA2, as well as p38-MAPK and c-Fos/AP-1 compared to *C. albicans*-yeast carriers or healthy patients. Furthermore, the activation of the p38-MAPK has also been directly associated with increased migration and proliferation of melanoma cells⁴⁶ and pancreatic cancer cells⁴⁷, in agreement with our results.

As expected, we confirmed that both the p38-MAPK and HIF-1 α participate, at least in part, in c-Fos gene and protein expression. Further studies will explore whether these two pathways are linked in these events. Any of the three MAPK pathways (ERK1/2, JNK and p38) can lead to HIF-1 α activation⁴⁸. Similarly high HIF-1 α activity is able to activate MAPK signaling⁴⁸. This could explain the impact of HIF-1 α on c-Fos expression, as already reported for c-Jun⁴⁹.

In our transcriptomic analysis the expression of other subunits of the AP-1 complex were found upregulated, specifically *Atf3*, *Jun*, and *Jund* genes. Further studies showed that all three genes and specifically *Jund* gene expression are regulated by both p38-MAPK and HIF-1 α , probably in the same fashion as *Fos*. However, similar to c-Fos, their expression was not totally repressed by p38-MAPK or HIF-1 α inhibitors, suggesting that a combination of processes are implicated in their induction. Some of these results align with those reported by Catar et al.⁵⁰ identifying the c-Fos/c-Jun AP-1 heterodimer complex as a critical regulator of VEGF release, with c-Fos playing a particularly prominent role in human vascular endothelial cells. Similar to our observations, they found that the expression of *FOS* was significantly higher than *JUN*. However, the impact of limited c-Fos or excess c-Jun on VEGF production remains to be fully elucidated⁵¹.

Apart from VEGF release, transcriptomic results indicated an upregulation of genes associated with aerobic glycolysis, suggesting that melanoma cells shift their metabolism towards this pathway in response to the fungus. To confirm this metabolic reprogramming, an ECAR assay was performed, which showed an increased acidification rate of the media as a result of lactate produced from pyruvate. Increased aerobic glycolysis has been often associated with the high energy demands that cancer cells present to support their migration, invasion, and proliferation⁵², but it has been also described in response to *C. albicans* in both non-tumor⁵³ and tumor¹¹ cell lines. Moreover, this process can be dependent on several mechanisms, including HIF-1 α and MAPKs⁵².

Therefore, we studied the relevance of this metabolic reprogramming in the release of VEGF stimulated by *C. albicans* on melanoma cells. Data showed a decrease in VEGF release when inhibiting the glycolytic enzyme HK2 and GLUT1, suggesting that the glycolytic pathway is necessary to maintain this response. Indeed, lactate, the end-product of aerobic glycolysis, is reported to play a key role in VEGF production⁵⁴⁻⁵⁷, and HIF-1 α accumulation⁵⁸. Moreover, it has been described that increasing lactate production promotes resistance of cancer cells to chemotherapy⁵⁹.

Finally, we investigated the role of the p38-MAPK and HIF-1 α on the expression of the genes involved in aerobic glycolysis *Hk2*, *Slc2a1*, and *Eno2*. Our results revealed that p38-MAPK upregulates *Eno2* and *Hk2* expression and *Slc2a1* to a lesser extent. Indeed, the involvement of p38-MAPK in the shift from oxidative phosphorylation to aerobic glycolysis has been observed in sepsis⁶⁰ and in pancreatic cancer cells⁴⁷. However, although HIF-1 α is frequently associated with the metabolic reprogramming in cancer cells⁶¹, we did not observe it in this case, and therefore, further studies will be needed to clarify this point.

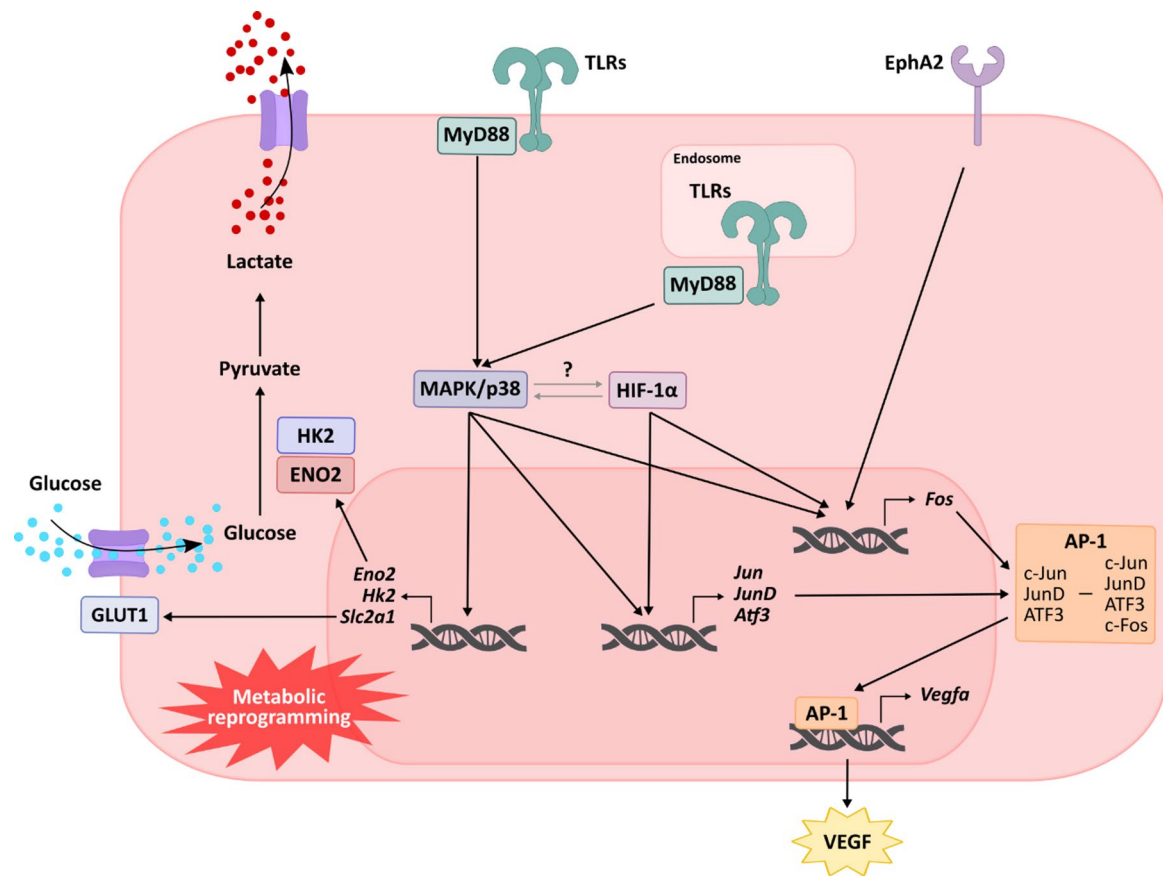


Fig. 7. Graphical representation of the hypothesized melanoma response to *C. albicans*. *C. albicans* is recognized by TLRs and EphA2, triggering VEGF release and c-Fos expression, respectively. Intracellularly, the p38 and HIF-1 α pathways are activated, promoting VEGF release through the activation of c-Fos/AP-1 and potentially other AP-1 subunits. Additionally, the p38 pathway plays a key role in driving metabolic reprogramming.

Despite the relevance of our findings, several limitations should be acknowledged. First, transcriptomic and functional analyses were restricted to a single time point, potentially overlooking earlier or later responses. Second, although murine cell lines and *in vivo* models provide valuable insights into cancer and metastasis, they cannot be directly extrapolated to human melanoma, as they have limitations such as the lack of common mutations (e.g., *BRAF*, *NRAS*) and response to widely used checkpoint inhibitors⁶².

Therefore, future studies should validate our findings in human-derived cells and employ models that better reflect the human tumor microenvironment, such as patient-derived organoids and xenografts. Moreover, it is important to determine how *C. albicans* influences immune infiltration and cytokine modulation *in vivo*, to test the impact of antifungal treatments on melanoma progression, and to investigate AP-1 complex formation and activity given its key role in tumor progression and therapeutic potential. These efforts should extend to other fungi, including *Malassezia*, the dominant skin genus in healthy individuals⁶³ and already linked to pancreatic cancer⁶⁴, as well as non-*albicans* *Candida* species (e.g., *C. tropicalis*, *C. dubliniensis*), which colonize multiple body sites, share traits with *C. albicans*, and may also promote tumorigenesis, as suggested by pan-cancer analyses of colorectal cancer samples⁵.

In conclusion, this study shows that *C. albicans* infection induces changes at the gene expression level in tumor cells, resulting in a more aggressive phenotype and the formation of a tumor microenvironment that would favor both the development and progression of cancer (Fig. 7). The fungus promotes melanoma cell migration, adhesion to LSECs, metastatic capacity, release of the pro-angiogenic VEGF, and metabolic reprogramming. Our data supports a model in which MyD88-mediated TLRs and EphA2 recognize *C. albicans* and induce VEGF release and c-Fos expression, respectively. Both p38-MAPK and HIF-1 α are activated, contributing to VEGF release via activation of c-Fos/AP-1 and possibly other AP-1 subunits, with p38-MAPK being responsible for the metabolic reprogramming. This, in turn, supports the maintenance of a pro-angiogenic microenvironment. Further studies will elucidate the mechanisms underlying the pro-tumor and pro-metastatic processes observed and potentially open the possibility of studying antifungal therapies as complement to traditional treatments for melanoma.

Methods

Microorganisms

Candida albicans CECT 13062 strain (Spanish Type Culture Collection), originated from a systemic candidiasis, was used with the approval of the Ethics Committee of the University of the Basque Country (UPV/EHU; M30/2019/114) and grown as previously described¹⁶. Briefly, the fungus was grown in Sabouraud Dextrose Agar (SDA) at 37 °C overnight. One day prior to the experiment, 10⁵ cells/mL were inoculated in Sabouraud Dextrose Broth (SDB) and incubated at 37 °C and 120 rpm overnight. The day of the experiment, yeasts were collected by centrifugation and washed twice with DPBS. Fungal cell numbers were calculated for each experiment using a hemocytometer.

All the experiments were carried out with live *C. albicans* unless otherwise specified. In order to obtain the inactive form of *C. albicans*, either yeast or hyphae, the fungus was heat-killed (HK-*C. albicans*) adjusting its concentration to 10⁷ cells/mL in DPBS and incubating for 30 min at 70 °C. Conditioned media was obtained by seeding 5 × 10⁵ melanoma cells/well in 12-well plates, stimulating them with live *C. albicans* at a MOI (*C. albicans*:melanoma cells) of 5 for six hours, and then collecting the supernatants, which were stored at –20 °C until further use.

Cells and culture conditions

B16-F10 melanoma cells (ATCC CRL-6475) and immortalized murine liver sinusoidal endothelial cells (LSECs; Innoprot Cat. # P10622) were kept in RPMI with 10% heat-inactivated fetal bovine serum (FBS), 2 mM L-glutamine, 100 U/mL penicillin, 100 µg/mL streptomycin and 0.25 µg/mL amphotericin B, in a 5% CO₂ atmosphere at 37 °C.

Wound healing assay

To evaluate cell migration, 1.5 × 10⁵ melanoma cells/well were seeded and cultured overnight in 24-well plates for obtaining a cell monolayer. The following day, a vertical and a horizontal scratch was made using a 1,000 µL pipette tip followed by two washing steps twice with DPBS to remove detached cells. Then, fresh media alone or with MOI 0.25 and 0.5 of live-*C. albicans* yeast was added to each well and inactivated after 6 h with 0.25 µg/mL amphotericin B. A Nikon Eclipse TE2000-U inverted microscope (Nikon) was utilized to photograph the same position of scratches at 0 and 24 h after scratching. The percentage of scratch reduction (i.e., wound closure) was calculated as: *Wound closure (%)* = [(Initial wound area – Final wound area)/Initial wound area] × 100, and normalized to the untreated control. Original, uncropped images are included in Supplementary Information.

Melanoma cells adhesion to LSECs assay

To study the effect of *C. albicans* on the adhesion capacity of melanoma cells to endothelial cells (LSECs) was done as previously described⁶⁵, with some modifications. Briefly, the day before the experiment 2.5 × 10⁵ LSECs/well were seeded in a 48-well plate and incubated overnight. Additionally, 1 × 10⁶ melanoma cells were seeded in 25 cm² cell culture flasks with or without HK-*C. albicans* yeast at MOI 10. The following day, melanoma cells were harvested and stained using 1 µM of carboxyfluorescein succinimidyl ester (CFSE; Invitrogen, Cat. # C34570) per 1 × 10⁶ cells in DPBS for 30 min, followed by washing in RPMI supplemented with 10% of FBS as previously described⁵⁹. Then, 2.5 × 10⁴ melanoma cells per well were added to the LSECs monolayers. The resulting co-cultures were maintained for 10 min at 37 °C and total emitted fluorescence was measured using Synergy HT (BioTek) with the Gen5 program (BioTek) and defined as initial fluorescence. Then, co-cultures were extensively but delicately washed with culture medium to prevent removing of adherent cells. The fluorescence emitted by adhered cells was again measured (final fluorescence). Finally, the percentage of adhered cells was calculated by the subtraction of background fluorescence (fluorescence emitted by LSECs alone) as: *Cell adhesion (%)* = [(Final fluorescence – Background fluorescence)/(Initial fluorescence – Background fluorescence)] × 100. Original, uncropped images are included in Supplementary Information.

Angiogenesis promotion assay

The pro-angiogenic microenvironment promotion was determined by seeding in 12-well plates 5 × 10⁵ melanoma cells/well with an MOI 5 of live *C. albicans* for six hours. The collected supernatant was then centrifuged to discard tumor and fungal debris, and the obtained conditioned media was stored at 4 °C with 0.25 µg/mL amphotericin B until the following day. In parallel, 1.25 × 10⁵ LSECs/well were seeded in 24-well cell culture plates overnight for obtaining cell monolayers. The following day, wound healing assays were performed as described above using the conditioned media stored as culture media and measuring wound closure percentage of LSECs after eight hours of exposure. Original, uncropped images are included as Supplementary File.

Cell proliferation assay

Cell proliferation assays by flow cytometry were performed in the Advanced Research Facilities from the UPV/EHU (SGIker) using a Beckman Coulter Gallios cytometer (Beckman Coulter).

Melanoma cells were first stained with the fluorescent dye CFSE as before. They were then resuspended in RPMI supplemented with 10% FBS and seeded at 2.5 × 10⁵ cells/well in 6-well plates. At 0 h, the cells were analyzed by flow cytometry using unstained cells as controls. The rest of the cells were exposed to fresh media alone or with MOI 1 and 10 of HK-yeast and after 24, 48 and 72 h, the cells were detached, resuspended in DPBS and analyzed in the same way. The flow cytometer was set up to analyze 10,000 events from each sample, exciting the sample at 492 nm and measuring the emitted fluorescence at 517 nm. Results were analyzed using Flowing Software 2 (<https://bioscience.fi/services/cell-imaging/flowing-software/>; Turku Bioscience Centre).

In vivo development of hepatic metastasis

The effect of *C. albicans* on the metastatic capacity of melanoma cells in vivo was studied using a murine hepatic metastasis model. All the in vivo experiments were performed in the Animal Unit Service of the SGiker. Syngeneic C57BL/6J mice (male, 6–8 weeks old) purchased from Janvier Labs were used. The authors confirm that all experiments were performed in accordance with relevant guidelines and regulations required by the Animal Experimentation Ethics Committee from the UPV/EHU (M20/2022/052).

First, 1×10^6 melanoma cells were seeded in 25 cm² cell culture flasks and incubated overnight. The following day, live *C. albicans* was added at MOI of 1 to the *C. albicans*-stimulated melanoma group. After six hours of co-incubation, melanoma cells of control and *C. albicans*-stimulated groups were detached from the flasks and adjusted to 1×10^6 cell/mL in DPBS supplemented with 25 µg/mL of amphotericin B in order to chemically inactivate the remaining *C. albicans*.

For the establishment of the hepatic metastasis, mice were first anesthetized using tiletamine-zolazepam at 80 mg/kg and xylazine at 10 mg/kg, and then, 1×10^5 melanoma cells/100 µl of DPBS per mouse, either previously stimulated with *C. albicans* or not, were injected intrasplenically. Mice were anesthetized as before and sacrificed by cervical dislocation 14 days after tumor cells injection (body weight of mice at time of euthanasia are included as Supplementary Table 1). The liver was then collected, fixed and paraffin-embedded for histological analyses after hematoxylin-eosin (H&E) staining. In the course of the experiment, the weight and symptoms of the mice complied with the ARRIVE guidelines. The macro- and microscopic regions of the liver occupied by tumor cells (tumor area) were quantified in the extracted organ and in 7 µm-thick tissue sections, respectively. Three different sections of each liver were evaluated allowing 500 µm separation between each of them. Liver tumor area was calculated as the area of metastatic foci per 200 mm² of liver section. This assay was performed twice with at least five mice per group. Original, uncropped images are included as Supplementary File.

RNA-seq and bioinformatic analysis

For transcriptomic analysis, 1×10^6 melanoma cells/well were seeded in 6-well plates, stimulated with MOI 1 of live *C. albicans* and after six hours total RNA isolation was performed by Total RNA Isolation Kit (NzyTech), following manufacturer's instructions. Total RNA quantity was measured using the Qubit RNA Assay Kit (Thermo Fisher Scientific) and its quality integrity was measured examined by RNA Nano Chips in a 2100 Bioanalyzer (Agilent Technologies) in the Center for Cooperative Research in Biosciences (CICBiogune) in Derio, Spain.

Then, RNA libraries were prepared with the TruSeq® Stranded mRNA Library Prep™ kit (Illumina Inc.) and TruSeq RNA Single Indexes (Illumina Inc.), Truseq RNA Sample Preparation Kit v2 (Illumina Inc.) and sequenced on HiScanSQ NovaSeq6000 Platform (Illumina Inc.) to generate 50 100 base single paired-end reads. The quality control of raw sequence data was performed using FastQC v.0.11.9.

Using STAR software⁶⁶, FASTQ files were aligned to Mouse genome data base mm10 and read counts obtained for each gene. Differential expression analysis was performed with the DESeq2 (data available through the Gene Expression Omnibus (<https://www.ncbi.nlm.nih.gov/geo/>) under accession number GSE285124).

The DEGs, GO and KEGG pathway enrichment analysis were determined using the online iDEP 1.0 tool (<http://149.165.154.220/idep10/>, BioMed Central Ltd, BCM Informatics) and Deseq2 method. For all of them the cut-off was assigned above the $|FC| > 1.5$ and a $p_{adj} < 0.05$. Further protein interaction networks studies were performed using the STRING tool. Furthermore, a second bioinformatics analysis of the results considering only the $p_{adj} < 0.05$ was also done.

Measurement of vascular endothelial growth factor (VEGF) release

For cytokine measurement, 5×10^5 melanoma cells/well were seeded in 12-well plates and stimulated with an MOI 5 of live *C. albicans*. After six hours the supernatants were collected and stored at -20 °C until use. ELISA assay to detect VEGF was performed using commercial VEGF-165 Mouse ELISA Development Kit (ABTS).

Gene expression measurement by RT-qPCR analysis

For RT-qPCR, 1×10^6 melanoma cells/well were seeded in 6-well plates, stimulated with an MOI of 5 of live *C. albicans* and after six hours total RNA was isolated and measured using the Nanodrop ND 1000 (Thermo Fisher Scientific) before being stored at -80 °C until used. cDNA was synthesized using the NZY First-Strand cDNA Synthesis Kit (NzyTech). RT-qPCR was performed using the NZYSupreme qPCR Green Master Mix (2x) (NzyTech) in a CFX96 Touch Real-Time PCR Detection System (Bio-Rad) thermal cycler. The primers used are listed in Supplementary Table 2. To determine the relative concentration of mRNAs relative to control the threshold cycle (Ct) values were normalized to the *Rpl19* housekeeping gene using the $\Delta\Delta Ct$ method.

Electrophoresis and Western blotting

The following experiments were performed as previously described¹⁶, with minor modifications. First, 5×10^5 melanoma cells/well in 12-well plates were seeded and stimulated for six hours with an MOI of 5 of live *C. albicans*. Protein extraction was performed using RIPA lysis buffer containing 1 mM protease inhibitors (Phenylmethylsulfonyl fluoride, PMSF) and incubated on ice for 10 min. Each well was then scrapped, collected, and incubated on ice another 10 min. Finally, the samples were centrifuged at maximum speed for 5 min and the supernatants stored at -20 °C until use.

For Western Blotting (WB), samples were loaded into 10% SDS-polyacrylamide gels and run at 70 mA, 100 W and 200 V for 45 min in a Miniprotean II (Bio-Rad), using the Page Ruler Plus protein standard. Proteins were then transferred to Hybond-P PVDF membranes (GE Healthcare, Cat. # RPN303F) for 1 h at 400 mA. Membranes were then blocked for 2 h with Tris Buffered Saline Milk (TBSM; 50 mM tris-HCl pH 7.5, 150 mM NaCl, 0.1% (v/v) Tween 20 and 5% (w/v) low fat dried milk, both from Sigma-Aldrich). Rabbit monoclonal

antibodies against c-Fos (YA506, Cat. # HY-P80081) and the housekeeping protein β -Tubulin (Cat. # HY-P80487) diluted 1:1,000 in TBSM were used as primary antibodies (MedChemExpress) and incubated with the membrane overnight at 4 °C. After three 5 min washes with TBS, goat anti-rabbit IgG (Thermo Fisher Scientific, Cat. # 31460) diluted 1:5,000 in TBSM was used as secondary antibody and incubated with the membrane for 30 min. All the steps were carried out at room temperature and agitation unless otherwise indicated. Membranes were developed using the NZY Standard ECL in a G: BOX Chemi system (Syngene). Densitometry analysis of WBs was performed using Image J (Bethesda). Original, uncropped Western Blots are included in Supplementary Information.

Inhibition of signaling and metabolic pathways

To inhibit different metabolic and signalling pathways, melanoma cells were treated with inhibitors for one hour at 37 °C and 5% CO₂ before *C. albicans* was added. The inhibitors of hexokinase (2-deoxyglucose, 2-DG, Cat # HY-1396; 5 mM), GLUT1 (BAY 876, Cat # HY-100017; 25 nM), SYK (Piceatannol, Cat # HY-13518; 30 μ M), MyD88 (TJ-M2010-5, Cat # HY-139397; 30 μ M), EGFR (PD153035, Cat # HY-14346; 1 μ M), EphA2 (NVP-BHG712, Cat # HY-13258 A; 1 μ M), ERK1/2 (PD-0325901, Cat # HY-10254; 1 μ M), JNK (SP600125, Cat # HY-12041; 10 μ M), p38a (SB 203580, Cat # HY-10256; 10 μ M), NF- κ B (BAY 11-7082, Cat # HY-13453; 2 μ M), c-Fos/AP-1 (T-5224, Cat # HY-12270; 10 μ M) and HIF-1 α (LW6, Cat # HY-13671; 10 μ M) were obtained from MedChemExpress.

Extracellular acidification rate (ECAR) assay

Glycolytic activity was assessed using the ECAR as a proxy, using the pH-Xtra Glycolysis Assay kit following the manufacturer's instructions, as previously described¹⁶. Briefly, 2.5×10^4 melanoma cells were seeded per well in black 96-well plates with clear bottoms and incubated overnight. The cells were washed twice with 100 μ L of pre-warmed respiration buffer adjusted to pH 7.4. After, 90 μ L of fresh respiration buffer was added to each well and immediately cells were infected with an MOI of 5 of live *C. albicans*. Finally, 10 μ L of pH-Xtra reagent was added to each well and the plates were incubated in the FlexStation 3 CO₂ free machine (Molecular Devices) for six hours at 37 °C, exciting the sample at 380 nm and measuring the fluorescence emitted by pH-Xtra reagent at 615 nm. For statistical analysis of the ECAR assay, the mean of the last five measurements (corresponding to the final 10 min) was calculated for each sample. The resulting values ($n = 4$ per group: control and infected with an MOI of 5 of live *C. albicans*) were then analyzed using an unpaired Student's t-test.

Statistical analysis

Each experiment were performed at least three times. Statistical analysis was conducted using the IBM SPSS statistical software (version 28.0.1.1; Professional Statistic). Experimental data were represented using GraphPad Prism 8.0 software. Two-tailed unpaired Student's t-test was performed to compare the means between two groups. Details of statistical analysis were mentioned in each Figure legends. The probability values of < 0.05 were considered statistically significant.

Preprint

A previous version of this manuscript was published as a preprint [Aparicio-Fernandez, L., et al. *Candida albicans* enhances melanoma cell aggressiveness through p38-MAPK and HIF-1 α pathways and metabolic reprogramming. Preprint at <https://doi.org/10.1101/2025.01.17.633543> (2025)].

Data availability

The authors confirm that the data supporting the findings of this study are available within the article and its supplementary materials. Raw data employed in the study (Source Data) is available also as Supplementary Information and the RNA-seq data through the Gene Expression Omnibus (<https://www.ncbi.nlm.nih.gov/geo/>) under the accession code GSE285124.

Received: 15 May 2025; Accepted: 10 October 2025

Published online: 17 November 2025

References

1. Sung, H. et al. Global cancer statistics 2020: GLOBOCAN estimates of incidence and mortality worldwide for 36 cancers in 185 countries. *CA Cancer J. Clin.* **71**, 209–249 (2021).
2. de Martel, C., Georges, D., Bray, F., Ferlay, J. & Clifford, G. M. Global burden of cancer attributable to infections in 2018: a worldwide incidence analysis. *Lancet Glob Health.* **8**, e180–e190. [https://doi.org/10.1016/S2214-109X\(19\)30488-7](https://doi.org/10.1016/S2214-109X(19)30488-7) (2020).
3. Dzutsev, A. et al. Microbes and cancer. *Annu. Rev. Immunol.* **35**, 199–228 (2017).
4. IARC (International Agency for Research on Cancer). Agents Classified by the IARC Monographs. 1–136. *World Health Organization* <https://monographs.iarc.who.int/agents-classified-by-the-iarc/> (2024).
5. Dohlman, A. B. et al. A pan-cancer mycobiome analysis reveals fungal involvement in Gastrointestinal and lung tumors. *Cell* **185**, 3807–3822e12. <https://doi.org/10.1016/j.cell.2022.09.015> (2022).
6. Narunskey-Haziza, L. et al. Pan-cancer analyses reveal cancer-type-specific fungal ecologies and bacteriome interactions. *Cell* **185**, 3789–3806e17. <https://doi.org/10.1016/j.cell.2022.09.005> (2022).
7. Liu, Z. et al. Intestinal *Candida albicans* promotes hepatocarcinogenesis by up-regulating NLRP6. *Front. Microbiol.* **13**, 812771. <https://doi.org/10.3389/fmicb.2022.812771> (2022).
8. Schille, T. B., Sprague, J. L., Naglik, J. R., Brunke, S. & Hube, B. Commensalism and pathogenesis of *Candida albicans* at the mucosal interface. *Nat. Rev. Microbiol.* **23**, 525–540. <https://doi.org/10.1038/s41579-025-01174-x> (2025).
9. Dawson, R. A. Leukoplakia and oral cancer. *J. R. Soc. Med.* **62**, 610–615 (1969).

10. Alnuaimi, A. D., Wiesenfeld, D., O'Brien-Simpson, N. M., Reynolds, E. C. & McCullough, M. J. Oral *Candida* colonization in oral cancer patients and its relationship with traditional risk factors of oral cancer: A matched case-control study. *Oral Oncol.* **51**, 139–145 (2015).
11. Vadovics, M. et al. *Candida albicans* enhances the progression of oral squamous cell carcinoma in vitro and in vivo. *mbio* **13**, e03144–e03121. <https://doi.org/10.1128/mBio.03144-21> (2022).
12. Cheng, Y., Ling, Z. & Li, L. The intestinal microbiota and colorectal cancer. *Front. Immunol.* **11**, 615056. <https://doi.org/10.3389/fimmu.2020.615056> (2020).
13. Ramirez-Garcia, A. et al. *Candida albicans* and cancer: can this yeast induce cancer development or progression? *Crit. Rev. Microbiol.* **42**, 181–193 (2016).
14. Wang, X. et al. Is *Candida albicans* a contributor to cancer? A critical review based on the current evidence. *Microbiol. Res.* **272**, 127370. <https://doi.org/10.1016/j.micres.2023.127370> (2023).
15. Zhu, Y. et al. Fungal-induced Glycolysis in macrophages promotes colon cancer by enhancing innate lymphoid cell secretion of IL-22. *EMBO J.* **40**, e105320. <https://doi.org/10.15252/embj.2020105320> (2021).
16. Aparicio-Fernandez, L. et al. *Candida albicans* increases the aerobic Glycolysis and activates MAPK-dependent inflammatory response of liver sinusoidal endothelial cells. *Microbes Infect.* **26**, 105305. <https://doi.org/10.1016/j.micinf.2024.105305> (2024).
17. Wang, X. et al. *Candida albicans* promotes oral cancer via IL-17A/IL-17RA-macrophage axis. *MBio* **14**, e0044723 (2023). 10.1128/mbio.00447-23.
18. Rodriguez-Cuesta, J. et al. *Candida albicans* enhances experimental hepatic melanoma metastasis. *Clin. Exp. Metastasis.* **27**, 35–42 (2010).
19. Ramirez-Garcia, A. et al. Molecular fractionation and characterization of a *Candida albicans* fraction that increases tumor cell adhesion to hepatic endothelium. *Appl. Microbiol. Biotechnol.* **92**, 133–145 (2011).
20. Ramirez-Garcia, A. et al. *Candida albicans* increases tumor cell adhesion to endothelial cells in vitro: intraspecific differences and importance of the mannose receptor. *PLoS One.* **8**, e53584. <https://doi.org/10.1371/journal.pone.0053584> (2013).
21. Szostak, N. et al. Gut mycobiota dysbiosis is associated with melanoma and response to anti-PD-1 therapy. *Cancer Immunol. Res.* **12**, 427–439 (2024).
22. d'Enfert, C. et al. The impact of the Fungus-Host-Microbiota interplay upon *Candida albicans* infections: current knowledge and new perspectives. *FEMS Microbiol. Rev.* **45**, fuaa060. <https://doi.org/10.1093/femsre/fuaa060> (2021).
23. Moyes, D. L. et al. A biphasic innate immune MAPK response discriminates between the yeast and hyphal forms of *Candida albicans* in epithelial cells. *Cell. Host Microbe.* **8**, 225–235 (2010).
24. Pellon, A., Nasab, S., Moyes, D. L. & S.D. & New insights in *Candida albicans* innate immunity at the mucosa: toxins, epithelium, metabolism, and beyond. *Front. Cell. Infect. Microbiol.* **10**, 81. <https://doi.org/10.3389/fcimb.2020.00081> (2020).
25. Song, D., Lian, Y. & Zhang, L. The potential of activator protein 1 (AP-1) in cancer targeted therapy. *Front. Immunol.* **14**, 1224892. <https://doi.org/10.3389/fimmu.2023.1224892> (2023).
26. Woo, Y. R., Cho, S. H., Lee, J. D. & Kim, H. S. The human microbiota and skin cancer. *Int. J. Mol. Sci.* **23**, 1813. <https://doi.org/10.3390/ijms23031813> (2022).
27. Hanahan, D. Hallmarks of cancer: new dimensions. *Cancer Discov.* **12**, 31–46 (2022).
28. Cho, W. C., Jour, G. & Aung, P. P. Role of angiogenesis in melanoma progression: update on key angiogenic mechanisms and other associated components. *Semin Cancer Biol.* **59**, 175–186 (2019).
29. Sprague, J. L. et al. *Candida albicans* translocation through the intestinal epithelial barrier is promoted by fungal zinc acquisition and limited by NF κ B-mediated barrier protection. *PLoS Pathog.* **20**, e1012031. <https://doi.org/10.1371/journal.ppat.1012031> (2024).
30. Nikou, S. A. et al. The *Candida albicans* toxin Candidalysin mediates distinct epithelial inflammatory responses through p38 and EGFR-ERK pathways. *Sci. Signal.* **15**, eabj6915. <https://doi.org/10.1126/SCISIGNAL.ABJ6915> (2022).
31. Moyes, D. L. et al. Candidalysin is a fungal peptide toxin critical for mucosal infection. *Nature* **532**, 64–68 (2016).
32. Swidergall, M. et al. Activation of EphA2-EGFR signaling in oral epithelial cells by *Candida albicans* virulence factors. *PLoS Pathog.* **17**, e1009221. <https://doi.org/10.1371/journal.ppat.1009221> (2021).
33. Russell, C. M. et al. Connecting the pore forming mechanism of this virulence factor to its immunostimulatory properties. *J. Biol. Chem.* **299**, 102829 (2022).
34. Moyes, D. L. et al. Protection against epithelial damage during *Candida albicans* infection is mediated by PI3K/Akt and mammalian target of Rapamycin signaling. *J. Infect. Dis.* **209**, 1816–1826 (2014).
35. Wang, W. et al. A small secreted protein triggers a TLR2/4-dependent inflammatory response during invasive *Candida albicans* infection. *Nat. Commun.* **10** <https://doi.org/10.1038/s41467-019-08950-3> (2019).
36. Lo, H. J. et al. Nonfilamentous *C. albicans* mutants are avirulent. *Cell* **90**, 939–949 (1997).
37. Qin, Y. et al. Innate immune cell response upon *Candida albicans* infection. *Virulence* **7**, 512–526 (2016).
38. Menden, H., Welak, S., Cossette, S., Ramchandran, R. & Sampath, V. Lipopolysaccharide (LPS)-mediated angiopoietin-2-dependent autocrine angiogenesis is regulated by NADPH oxidase 2 (Nox2) in human pulmonary microvascular endothelial cells. *J. Biol. Chem.* **290**, 5449–5461 (2015).
39. Swidergall, M., Solis, N. V., Lionakis, M. S. & Filler, S. G. EphA2 is an epithelial cell pattern recognition receptor for fungal β -glucans. *Nat. Microbiol.* **3**, 53–61 (2018).
40. Müller, V. et al. *Candida albicans* triggers activation of distinct signaling pathways to Establish a Proinflammatory gene expression program in primary human endothelial cells. *J. Immunol.* **179**, 8435–8445 (2007).
41. Yang, J. et al. *Candida albicans* triggers the expression of inflammatory genes in human umbilical vein endothelial cells. *Exp. Ther. Med.* **12**, 1490–1494 (2016).
42. Li, T. et al. HSPA12A stimulates p38/ERK-AP-1 signaling to promote angiogenesis and is required for functional recovery postmyocardial infarction. *Oxid. Med. Cell. Longev.* **2022** (2333848). <https://doi.org/10.1155/2022/2333848> (2022).
43. Ahmad, A. & Nawaz, M. I. Molecular mechanism of VEGF and its role in pathological angiogenesis. *J. Cell. Biochem.* **123**, 1938–1965 (2022).
44. Moyes, D. L. et al. *Candida albicans* yeast and hyphae are discriminated by MAPK signaling in vaginal epithelial cells. *PLoS One.* **6**, e26580. <https://doi.org/10.1371/journal.pone.0026580> (2011).
45. Roselletti, E., Perito, S., Sabatini, S., Monari, C. & Vecchiarelli, A. Vaginal epithelial cells discriminate between yeast and hyphae of *Candida albicans* in women who are colonized or have vaginal candidiasis. *J. Infect. Dis.* **220**, 1645–1654 (2019).
46. Estrada, Y., Dong, J. & Ossowski, L. Positive crosstalk between ERK and p38 in melanoma stimulates migration and in vivo proliferation. *Pigment Cell. Melanoma Res.* **22**, 66–76 (2009).
47. Wang, F. et al. p38 MAPK is essential for aerobic Glycolysis and pancreatic tumorigenesis. *Cancer Res.* **80**, 3251–3264 (2020).
48. Korbecki, J. et al. Chronic and cycling hypoxia: drivers of cancer chronic inflammation through Hif-1 and Nf- κ b activation. A review of the molecular mechanisms. *Int. J. Mol. Sci.* **2**, 10701. <https://doi.org/10.3390/ijms221910701> (2021).
49. Laderoute, K. R. et al. The response of c-Jun/AP-1 to chronic hypoxia is hypoxia-inducible factor 1 α dependent. *Mol. Cell. Biol.* **22**, 2515–2523 (2002).
50. Catar, R. et al. Transcriptional regulation of thrombin-induced endothelial VEGF induction and proangiogenic response. *Cells* **10**, 910. <https://doi.org/10.3390/cells10040910> (2021).
51. Bonder, C. S. & Ebert, L. M. Fos-icting for control of angiogenesis: increasing the longevity of peritoneal Dialysis. *Kidney Int.* **84**, 1065–1067 (2013).

52. Schiliro, C. & Firestein, B. L. Mechanisms of metabolic reprogramming in cancer cells supporting enhanced growth and proliferation. *Cells* **10**, 1056 (2021).
53. Pellon, A. et al. Fungal infection drives metabolic reprogramming in epithelial cells via aerobic glycolysis and an alternative TCA cycle shunt. <https://www.researchsquare.com/article/rs-2159406/v1> (2022).
54. Zhang, Y. et al. The function and mechanism of lactate and lactylation in tumor metabolism and microenvironment. *Genes Dis.* **10**, 2029–2037 (2023).
55. Polet, F. & Feron, O. Endothelial cell metabolism and tumour angiogenesis: glucose and glutamine as essential fuels and lactate as the driving force. *J. Intern. Med.* **273**, 156–165 (2013).
56. Kumar, V. B. S., Viji, R. I., Kiran, M. S. & Sudhakaran, P. R. Endothelial cell response to lactate: implication of PAR modification of VEGF. *J. Cell. Physiol.* **211**, 477–485 (2007).
57. Beckert, S. et al. Lactate stimulates endothelial cell migration. *Wound Repair. Regen.* **14**, 321–324 (2006).
58. Lu, H., Forbes, R. A. & Verma, A. Hypoxia-inducible factor 1 activation by aerobic Glycolysis implicates the Warburg effect in carcinogenesis. *J. Biol. Chem.* **277**, 23111–23115 (2002).
59. Qu, J. et al. *C. tropicalis* promotes chemotherapy resistance in colon cancer through increasing lactate production to regulate the mismatch repair system. *Int. J. Biol. Sci.* **17**, 2756–2769 (2021).
60. Mager, C. E. et al. p38 MAPK and MKP-1 control the glycolytic program via the bifunctional Glycolysis regulator PFKFB3 during sepsis. *J. Biol. Chem.* **299**, 103043. <https://doi.org/10.1016/j.jbc.2023.103043> (2023).
61. Jaworska, M. et al. The Warburg effect: a score for many instruments in the concert of cancer and cancer niche cells. *Pharmacol. Rep.* **75**, 876–890 (2023).
62. Zhong, W. et al. Comparison of the molecular and cellular phenotypes of common mouse syngeneic models with human tumors. *BMC Genom.* **21** (2). <https://doi.org/10.1186/s12864-019-6344-3> (2020).
63. Findley, K. et al. Topographic diversity of fungal and bacterial communities in human skin. *Nature* **498**, 367–370 (2013).
64. Aykut, B. et al. The fungal mycobiome promotes pancreatic oncogenesis via activation of MBL. *Nature* **574**, 264–267 (2019).
65. Benedicto, A. et al. Liver sinusoidal endothelial cell ICAM-1 mediated tumor/endothelial crosstalk drives the development of liver metastasis by initiating inflammatory and angiogenic responses. *Sci. Rep.* **13** 111 <https://doi.org/10.1038/s41598-019-49473-7> (2019).
66. Dobin, A. et al. Ultrafast universal RNA-seq aligner. *Bioinformatics* **29**, 15–21 (2013).

Acknowledgements

This work was supported by the Basque Government (Grant numbers IT1362-19 and IT1657-22). The CIC bio-GUNE support was provided by the Basque Department of Industry, Tourism and Trade (Etortek, Elkartek and Emaitek Programs), the Innovation Technology Department of Bizkaia County, CIBERehd Network, and Spanish MINECO the Severo Ochoa Excellence Accreditation [CEX2021-001136-S]. LM-S, MA, OR-E and LA-D have received a predoctoral grant from the Basque Government and LA-F from the University of the Basque Country (UPV/EHU). AP was supported by a fellowship from the Basque Government Postdoctoral Program. The authors declare that no funds, grants, or other support were received during the preparation of this manuscript. The authors thank for technical and human support provided by SGIker (UPV/EHU/ ERDF, EU) in the animal experimentation and flow citometry analysis performed.

Author contributions

L. A.-F. : Conceptualization, Data curation, Formal analysis, Investigation, Methodology, Validation, Visualization, Writing – original draft. N. C.-B. : Formal analysis, Investigation. M. A., O. R.-E., L. A.-D., L. M.-S. and I. B. : Investigation. J. M. and B. (A) : Investigation, Resources. A. (B) : Data curation, Formal analysis, Investigation, Resources. N. M.-C. and M. G. : Investigation. J. E. M. R. : Investigation, Software. A. M. Ar. : Data curation, Formal analysis, Funding acquisition, Investigation, Resources, Software, Validation. A. P. : Formal analysis, Investigation. D. L. M. : Resources, Supervision, Validation. J. A. : Formal analysis, Funding acquisition, Resources, Software, Supervision, Validation. A. R. and A. R.-G. : Conceptualization, Funding acquisition, Methodology, Project administration, Resources, Supervision. A. An. : Conceptualization, Data curation, Formal analysis, Methodology, Project administration, Supervision, Validation, Writing – original draft. All authors reviewed the manuscript and agree with its submission for publication.

Declarations

Competing interests

The authors declare no competing interests.

Ethics declarations

The study has obtained approval from the Ethics Committee of the University of the Basque Country (UPV/EHU) for the use of microorganisms, with the Ethics Approval Number being M30/2019/114. Moreover, all the *in vivo* experiments were performed in the Animal Unit Service of the SGIker and were approved by the Animal Experimentation Ethics Committee from the UPV/EHU with the Ethics Approval Number being M20/2022/052. All ethical regulations to animal research were followed.

Additional information

Supplementary Information The online version contains supplementary material available at <https://doi.org/10.1038/s41598-025-24055-y>.

Correspondence and requests for materials should be addressed to A.A.

Reprints and permissions information is available at www.nature.com/reprints.

Publisher's note Springer Nature remains neutral with regard to jurisdictional claims in published maps and institutional affiliations.

Open Access This article is licensed under a Creative Commons Attribution-NonCommercial-NoDerivatives 4.0 International License, which permits any non-commercial use, sharing, distribution and reproduction in any medium or format, as long as you give appropriate credit to the original author(s) and the source, provide a link to the Creative Commons licence, and indicate if you modified the licensed material. You do not have permission under this licence to share adapted material derived from this article or parts of it. The images or other third party material in this article are included in the article's Creative Commons licence, unless indicated otherwise in a credit line to the material. If material is not included in the article's Creative Commons licence and your intended use is not permitted by statutory regulation or exceeds the permitted use, you will need to obtain permission directly from the copyright holder. To view a copy of this licence, visit <http://creativecommons.org/licenses/by-nc-nd/4.0/>.

© The Author(s) 2025